ACS APPLIED MATERIALS & INTERFACES

Organic Electronic Devices

Improving the Electronic Transporting Property for Flexible Field-effect Transistor with Naphthalene Diimide-based Conjugated Polymer through Branching/linear Side-chain Engineering Strategy

Jing Ma, Zhiyuan Zhao, Yunlong Guo, Hua Geng, Yanan Sun, Jianwu Tian, Qiming He, Zhengxu Cai, Xisha Zhang, Guanxin Zhang, Zitong Liu, Deqing Zhang, and Yunqi Liu

ACS Appl. Mater. Interfaces, **Just Accepted Manuscript** • DOI: 10.1021/acsami.9b00531 • Publication Date (Web): 09 Apr 2019

ACS Publications

is published by the American Chemical Society. 1155 Sixteenth Street N.W., Washington, DC 20036

Improving the Electronic Transporting Property for Flexible Field-effect Transistor with Naphthalene Diimide-based Conjugated Polymer through Branching/linear Side-chain Engineering Strategy

Jing Ma,[†‡§] Zhiyuan Zhao,[†§] Yunlong Guo,[†] Hua Geng,[※] Yanan Sun,[※] Jianwu Tian,[†‡] Qiming He,[#] Zhengxu Cai,[//] Xisha Zhang,[‡] Guanxin Zhang,[†] Zitong Liu,[†] Deqing Zhang,*[†‡] Yunqi Liu[†]*

[†]Beijing National Laboratories for Molecular Sciences, CAS Key Laboratories of Organic Solids, CAS Research/Education Center for Excellence in Molecular Sciences, Institute of Chemistry, Chinese Academy of Sciences, Beijing 100190, P. R. China

[‡]University of Chinese Academy of Sciences, Beijing 100049, P. R. China

[#]Institute for Molecular Engineering, The University of Chicago, 5640 South Ellis Avenue, Chicago, Illinois 60637, United States

[||]Beijing Key Laboratory of Construction Tailorable Advanced Functional Materials and Green Applications, School of Material Science & Engineering, Beijing Institute of Technology, Beijing 100081, China

[※]Department of Chemistry, Capital Normal University, Beijing, 100048, P.R. China.

[§]These authors contributed equally to this work

Keywords: *n*-type polymeric semiconductor; conjugated polymer; naphthalene diimide; side chain; flexible field-effect transistor

Abstract

n-Type organic/polymeric semiconductors with high electron mobilities are highly demanded for future flexible organic circuits. Except for developing new conjugated backbone, recent studies show that side-chain engineering also plays an indispensable role in boosting the charge transporting property. In this paper, we report a new polymer **PNDI2T-DTD** with a representative *n*-type naphthalene diimide (NDI)-bithiophene backbone for high-performance *n*-type flexible thin film transistors through branching/linear side-chain engineering strategy. Serving as the flexible side chains, the linear/branching side chain pattern is found to effective in tuning the pre-aggregation behavior in solution and the packing ordering of polymeric chains, resulting in the improvement of thin film crystallinity. The electron mobility of the thin film of **PNDI2T-DTD** on flexible substrates can reach 1.52 $cm^2V^{-1}s^{-1}$, which is approximately five times higher than that of **PNDI2T-DT** with the same conjugated backbone and only branching alkyl chains.

Introduction

Semiconducting conjugated polymers show good solution rheology and mechanical properties as well as good compatibility with plastic substrates.[1–4] Therefore, field-effect transistors with polymeric semiconductors (PFETs) and integrated circuits can be utilized for flexible electronics such as flexible wearable sensors and electronic skin, large area displays, and memory devices.[5–9] Over the past decades, a number of conjugated polymers have been designed and investigated for PFETs with high semiconducting performances.[10–21] However, most of them exhibit *p*-type semiconducting behaviors, while the development of unipolar *n*-type polymeric semiconductors lags far behind the *p*-type ones. Although many *n*-type semiconducting polymers have been

reported recently, most of PFETs based on them are fabricated on rigid substrates and measured under inert atmosphere or even vacuum.[11,12,16,17] Moreover, the PFETs with certain semiconducting polymers show low *on/off* ratios (even less than 10^3) because these polymers not only show *n*-type characteristics, but also weak *p*-type transporting behaviors.[22–24] In fact, PFETs fabricated from unipolar *n*-type conjugated polymers, possessing both satisfying electron mobility, high *on/off* ratio and good air stability, are urgently demanded.

Among the *n*-type conjugated D–A polymers, naphthalene-diimide (NDI)-based copolymers have been extensively investigated.[3, 25–35] This is owing to the unique advantages of NDI, including i) highly electron-deficient characteristics of NDI with good planarity, ii) good solubility after incorporation of alkyl chains at the nitrogen-positions and iii) excellent thermal stability. To date, various NDI-based copolymers with various electron donors, such as thiophene,[26] selenophene,[34] thiophen-vinyl-thiophene,[30] and bithiophene,[31–32] have been investigated. For instance, some of us reported NDI-selenophene copolymers exhibiting electron mobility up to 8.5 $cm^2V^{-1}s^{-1}$ on OTS-modified SiO_2/Si substrate.[34] Later, Michinobu, Wang and their coworkers prepared NDI-based copolymer entailing benzothiadiazole units in the backbone and the resulting PFET on amine-tailed self-assembly monolayer modified SiO_2/Si substrate exhibited electron mobility up to 5.35 $cm^2V^{-1}s^{-1}$ in vacuum.[35] In comparison, *n*-type PFETs with conjugated copolymers on flexible substrates were less explored. The surface of flexible substrate is usually not smooth, which can affect the packing of polymer chains. Facchetti and co-workers once reported *n*-type FETs (field-effect transistors) with NDI-bithiophene copolymer on flexible PET (polyethylene terephthalate) substrate with maximum electron mobility of 0.65 $cm^2V^{-1}s^{-1}$,[3] being much lower than those for thin films of the same polymer on solid substrates.[36–39] Since then, the NDI-bithiophene skeleton polymers have become benchmarks in organic

semiconductor including PFETs and organic solar cells.[30–32] The simple structure and accessible precursors make them more promising for future applications. Hence, development of NDI-based polymers with high electron mobilities on flexible substrate is an urgent task.

In this paper, we report *n*-type FETs on flexible polyethylene terephthalate (PET) substrate with electron mobility up to 1.52 $cm^2V^{-1}s^{-1}$ and *on/off* ratios reaching 10^5 by using new NDI-based copolymer **PNDI2T-DTD** through branching/linear side-chain engineering strategy (**Scheme 1**). The conjugated backbone of **PNDI2T-DTD** contains representative alternating NDI and bithiophene units as in **PNDI2OD-T2**.[3] Each NDI unit in **PNDI2T-DTD** is connected to one branching and one linear alkyl chains at the *N, N'*-positions. It is noted that long branching alkyl chains (2-decyltetradecyl) can endow **PNDI2T-DTD** with good solubilities, while linear alkyl chain (*n*-dodecyl) can improve the planarity of conjugated backbone by reducing the steric hindrance and promoting interchain interdigitation and thus dense interchain packing. As a result, thin film of **PNDI2T-DTD** shows better crystallinity based on GIWAXS data and approximately five times higher electron mobility than that of NDI-based copolymer **PNDI2T-DT** with the same conjugated backbone as **PNDI2T-DTD**, but with two branching chains. We believe that the better crystallinity is attributed to the strong interchain pre-aggregation of **PNDI2T-DTD** in solutions, affecting the surface orientation of conjugated polymers on substrates and thus the semiconducting properties. These results demonstrate that this branching/linear side-chain engineering strategy is an efficient approach to modulate the interchain packing modes and boost the *n*-type semiconducting performances of conjugated polymers.

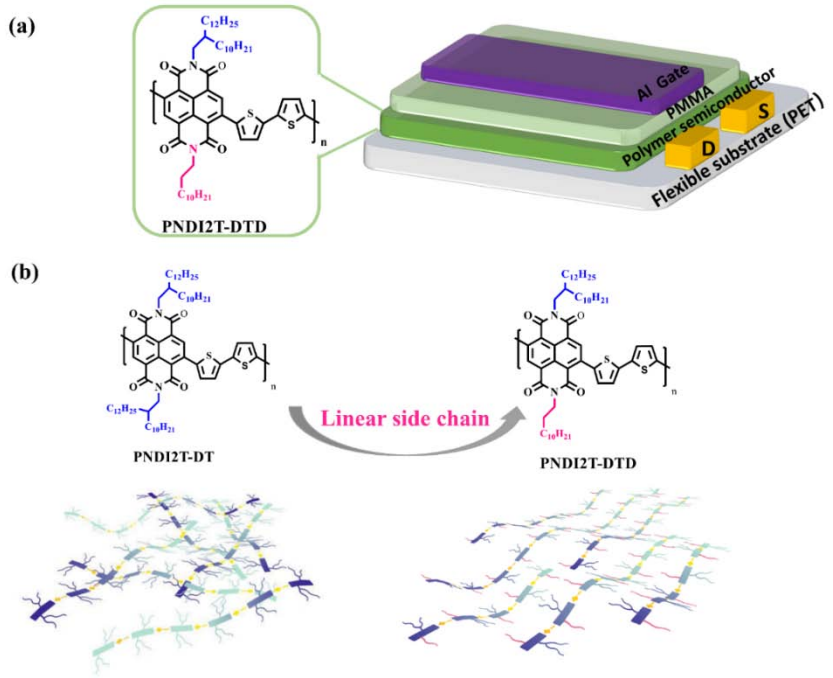

Scheme 1. (a) Chemical structure of **PNDI2T-DTD** and schematic illustration of top-gated FET device structure. (b) Schematic illustration of the branching/linear side-chain engineering strategy which can reduce the steric crowding of branching alkyl chains and improve interchain packing order.

Results and Discussion

Synthesis and Characterization

Synthesis of copolymer **PNDI2T-DTD** is shown in the Supporting Information. For comparison, copolymer **PNDI2T-DT** with the same backbone as of **PNDI2T-DTD** with two branching alkyl chains at the *N, N'*-positions was also prepared. The syntheses and characterizations of monomers are provided in the Supporting Information. The Stille coupling of monomer **1** with distannylated bithiophene yielded copolymer **PNDI2T-DTD** in 87% yield after purification by Soxhlet extraction with different organic solvents to remove remaining monomers, oligomers, and other side products. **PNDI2T-DT** was prepared following the same

procedure. Copolymers **PNDI2T-DTD** and **PNDI2T-DT** were characterized with high temperature ^{1}H NMR and elemental analysis. The M_ws (weight-average molecular weights) and PDIs (polydispersity indexes) determined by high temperature gel permeation chromatography were measured to be 45 and 37 kDa with PDI = 2.1 and 2.4 for **PNDI2T-DTD** and **PNDI2T-DT**, respectively. The decomposition temperatures of **PNDI2T-DTD** and **PNDI2T-DT** were measured to be 470 ^{o}C and 467 ^{o}C (5% weight loss) based on the thermogravimetric analysis (TGA, **Figure S1**). Thus, both copolymers are thermally stable under ca. 470 ^{o}C. No obvious thermal transitions were observed in the DSC curves (**Figure S2**). While **PNDI2T-DT** exhibits good solubility (higher than 10 mg/mL) in 1,2-dichlorobenzene, **PNDI2T-DTD** shows poor solubility (less than 1 mg/mL) in 1,2-dichlorobenzene at room temperature.

Electrochemical and Optical Properties

Cyclic voltammogram of **PNDI2T-DTD** was measured (**Figure S3**). The onset potentials (oxidation and reduction) were 1.01 and -0.89 V in reference to the redox potential of ferrocence ($E^{1/2}$ (Fc/Fc$^+$)). Accordingly, the HOMO/LUMO energies of **PNDI2T-DTD** were estimated to be -5.81/-3.91 eV (**Table 1**). Similarly, on the basis of the onset oxidation and reduction potentials of **PNDI2T-DT**, its HOMO/LUMO energies were estimated to be -5.88/-3.88 eV. The LUMO is slightly lowered and the HOMO is enhanced for thin film of **PNDI2T-DTD** compared to those of **PNDI2T-DT**.

Thin film of **PNDI2T-DTD** shows strong absorption around 714 nm with a shoulder peak at 781 nm, which is slightly red-shifted compared to the thin film absorption maximum of **PNDI2T-DT**, as shown in **Figure 1a**. Based on the thin film onset absorptions, the optical bandgap of **PNDI2T-DTD** and **PDNI2T-DT** were estimated to be 1.41 and 1.42 eV, respectively.

Table 1. Absorption maxima, redox potentials, HOMO/LUMO energies, and bandgaps of **PNDI2T-DTD** and **PNDI2T-DT**.

Polymer	λ_{max}[a] (nm)		E_{red}^{onset} (V)[b]	E_{ox}^{onset} (V)[b]	*experimental(calcd.)*[e]		E_g^{cv} (eV)[c]	E_g^{opt} (eV)[d]
	solution	thin film			LUMO (eV)	HOMO (eV)		
PNDI2T-DTD	392, 715	398,714	-0.89	1.01	-3.91(-3.47)	-5.81(-5.56)	1.90	1.41
PNDI2T-DT	368, 614	392, 696	-0.92	1.08	-3.88(-3.45)	-5.88(-5.61)	2.00	1.42

[a] Absorption maxima; [b] Onset potentials (V vs Fc/Fc^+); [c] Based on redox potentials; [d] Based on absorption spectral data; [e] DFT calculations for the respective dimers.

Interestingly, the absorption maximum of **PNDI2T-DTD** (715 nm) in 1,2-dichlorobenzene (10^{-2} mg/mL) was largely red-shifted by 101 nm compared to that of **PNDI2T-DT** as shown in **Figure 1b**. Considering the fact that **PNDI2T-DTD** and **PNDI2T-DT** possess the same conjugated backbone and have different side alkyl chains, we hypothesized that such large spectral shift can be attributed to pre-aggregation of polymer chains of **PNDI2T-DTD** in solution. The possible steric hindrance due to the branching alkyl chains along the conjugated backbone can be reduced by replacement with linear ones, and accordingly the planarity of the conjugated backbone can be improved. The backbone planarity of **PNDI2T-DTD** was also confirmed by DFT calculations (see below). The planar backbone of is beneficial for the pre-aggregation of **PNDI2T-DTD** in solution. The pre-aggregation of polymer chains of **PNDI2T-DTD** in solution was experimentally confirmed by the absorption spectra of **PNDI2T-DTD** in 1,2-dichlorobenzene at different temperatures. **Figure 1c** shows gradual blue shift in the absorption spectrum of **PNDI2T-DTD** by increasing the solution temperature from 25 ^oC to 120 ^oC. Pre-aggregation in solution is known to efficiently affect the packing order of conjugated polymer and thus the semiconducting properties.[40–42] Moreover, the pre-aggregation of polymer chains in solution may avoid the further self-assembly of polymer chains on flexible polymer

substrates. This feature is expected to be beneficial for the fabrication of flexible FETs as discussed below.

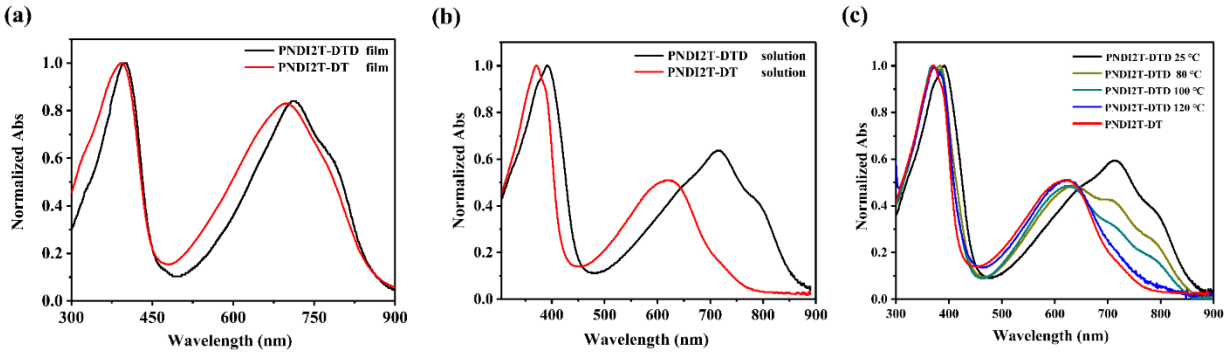

Figure 1. Normalized absorption spectra of **PNDI2T-DTD** and **PNDI2T-DT** in their thin films (a) and 1,2-dichlorobenzene solutions (10^{-2} mg/mL) at room temperature (b) as well as those of **PNDI2T-DTD** in 1,2-dichlorobenzene solutions at different temperatures (c).

Theoretical calculation

In order to investigate the influence of the linear side chains, DFT calculations for **PNDI2T-DTD** and **PNDI2T-DT** were carried out (see **Figure 2**). For simplicity, two-repeated units of **PNDI2T-DTD** and **PNDI2T-DT** were calculated. The dihedral angle between two NDI units was employed to estimate the planarity of polymer backbones. For **PNDI2T-DTD**, the twist angle of two NDI units was calculated to be 27.7°, which decreased significantly compared to that of **PNDI2T-DT** (76.5°) calculated with PM6/3-21G(d,p). Obviously, introducing linear side chains in polymer backbone significantly improves the conjugated backbone planarity, which is beneficial for both intra- and interchain charge transporting.

The long side chains in the optimized configurations were replaced by methyl groups and the frontier orbital energies were calculated with B3LYP/6-31G(d,p). The HOMO/LUMO orbitals were calculated to be -5.56/-3.47 eV for the dimer of **PNDI2T-DTD** and -5.61/-3.45 eV for the

dimer of the reference polymer **PNDI2T-DT**. This agrees well with the absorption spectral and cyclic voltammetric data which indicate that **PNDI2T-DTD** and **PNDI2T-DT** possess similar frontier orbital (HOMO/LUMO) energies (see **Table 1**). These calculations show that the replacement of branching alkyl chains with the linear alkyl chains do not have a significant influence on frontier orbital energies of **PNDI2T-DTD**. This may be explained by considering that the HOMO and LUMO energy levels of conjugated donor-acceptor polymers are related to the super-exchange coupling.[43] As shown in **Figure 2**, the frontier orbital charge densities at the donor and acceptor linkage sites have negligible distribution for the respective dimers of **PNDI2T-DTD** and **PNDI2T-DT**. Accordingly, the super-exchange coupling becomes weakly dependent on the dihedral angles. Thus, it is not unexpected that the calculated frontier orbital energies of the dimers of **PNDI2T-DTD** and **PNDI2T-DT** are rather similar although the conjugated backbone of **PNDI2T-DTD** is more planar.

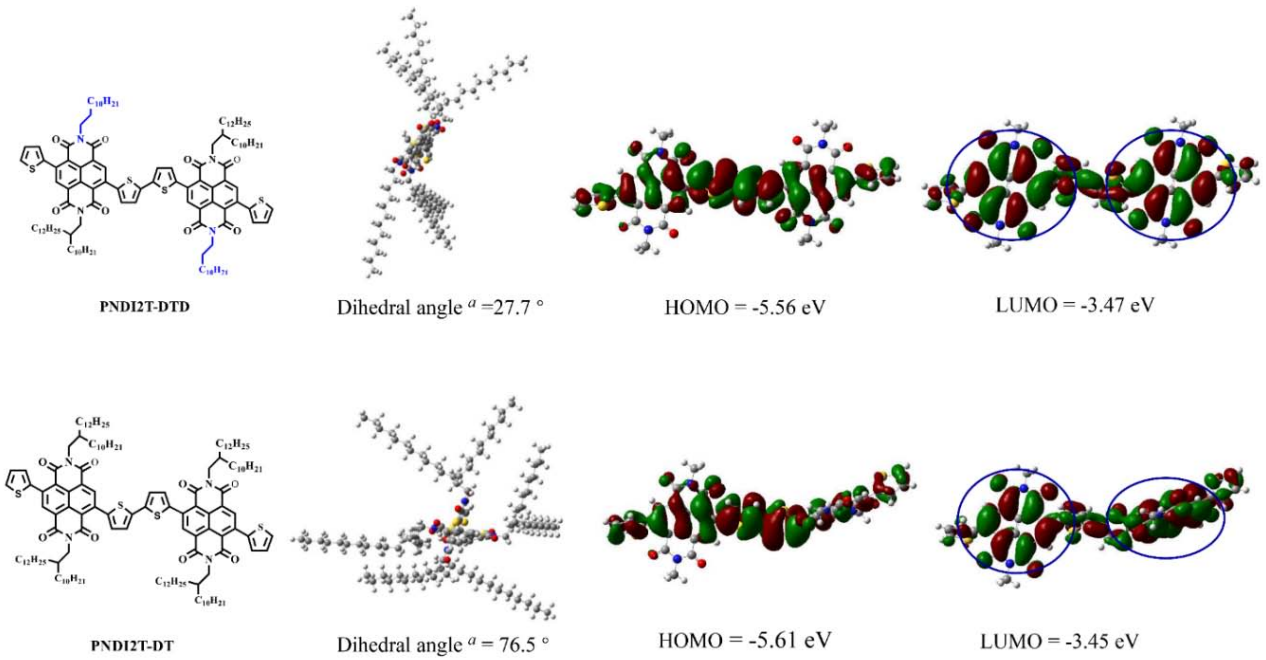

Figure 2. The calculated dihedral angles between the two neighboring NDI units and frontier orbital energies for the two repeated units of **PNDI2T-DTD** (*up*) and **PNDI2T-DT** (*down*).

Charge-transporting properties of FETs

Thin films of **PNDI2T-DTD** were utilized to fabricate top-gate/bottom-contact (TGBC) FETs with a device structure of polyethylene terephthalate (PET)/Au/**PNDI2T-DTD**/poly (methyl methacrylate) (PMMA)/Al. The devices were fabricated in glove-box (nitrogen), and then their charge transporting characteristics were measured under ambient conditions. Thin films were prepared by spin-coating of the **PNDI2T-DTD** solution in 1,2-dichlorobenzene (3 mg/mL) on PET substrates containing source and drain electrodes, followed by thermal annealing at 160 ^{o}C to remove the solvent residues. After that, PMMA was deposited on to the thin films as a dielectric and encapsulation layer for the devices (for details, see the Supporting Information).[44] For comparison, FETs with thin films of **PNDI2T-DT** on PET substrates were also fabricated similarly.

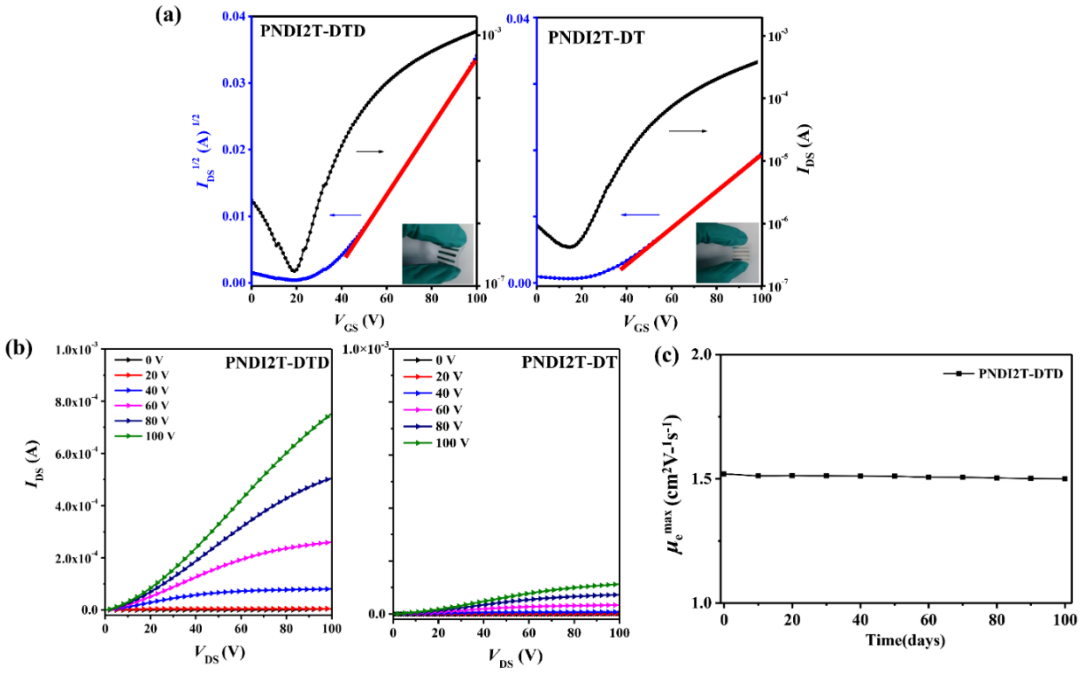

Figure 3. Transfer (V_{DS} = 100 V) (a) and output (b) characteristics of **PNDI2T-DTD** and **PNDI2T-DT** fabricated on PET devices measured in air with TGBC structure (W= 4500 μm, L = 30 μm). (c) The variation of electron mobility for the FET with thin film of **PNDI2T-DTD** which was stored in air with 15% humidity for 100 days.

Figure 3 shows the typical transfer and output curves of thin film FETs of **PNDI2T-DTD** and **PNDI2T-DT**. As expected, the thin films of both **PNDI2T-DTD** and **PNDI2T-DT** exhibit dominant *n*-channel transporting characteristics. The corresponding FET performance data, including electron mobilities, threshold voltages, *on/off* current ratios (I_{on}/I_{off}), and sub-threshold swings (*SS*), are listed in **Table 2**. For comparison, the semiconducting performance data for the bottom-gate top-contact FETs on rigid substrate with **PNDI2T-DT**[31] were also included in **Table 2**, while **Table S1** summarized the performances of the recently reported *n*-type FETs on flexible substrates with polymeric semiconductors. The average electron mobility (μ_e^{ave}) of thin film of **PNDI2T-DTD** on PET substrate can reach 1.34 $cm^2V^{-1}s^{-1}$ with the μ_e^{max} up to 1.52 $cm^2V^{-1}s^{-1}$, being about six times higher than μ_e^{ave} (0.23 $cm^2V^{-1}s^{-1}$) of **PNDI2T-DT**. By following the recent report,[45] the effective electron mobilities for FETs with thin films of **PNDI2T-DTD** and **PNDI2T-DT** were calculated and listed in **Table 2** (for details, see Supporting Information). The FET with **PNDI2T-DTD** on PET substrate also shows higher electron mobility than that with **PNDI2T-DT** OTS-modified SiO_2/Si rigid substrate (see **Table 2**).[31] Moreover, FETs with thin films of **PNDI2T-DTD** show high *on/off* ratio up to 10^5 in the saturation regime by comparing to those ($I_{on}/I_{off} = 10^3$) of FETs with **PNDI2T-DT**. As discussed below, the superior semiconducting performance of **PNDI2T-DTD** over **PNDI2T-DT** can be attributed to the improvement of thin film crystallinity after introducing the linear chain for each NDI unit in **PNDI2T-DTD**. Furthermore, the electron mobility of the flexible FETs with **PNDI2T-DTD** remained to be 1.50 $cm^2V^{-1}s^{-1}$ after the devices were stored under ambient conditions for 100 days (**Figure 3c**). Therefore, FETs with **PNDI2T-DTD** on PET substrates exhibit good air-stability. In addition, mechanical bending experiments (see Supporting Information) demonstrate

that the semiconducting performances of FETs with **PNDI2T-DTD** on flexible substrate are stable after mechanical bending.

Table 2. The electron mobilities, threshold voltages (V_{th}), *on/off* current ratios (I_{on}/I_{off}), and sub-threshold swings (*SS*) for thin-film FETs of **PNDI2T-DT** and **PNDI2T-DTD**.[a]

polymer	μ_e^{max}($cm^2V^{-1}s^{-1}$)	μ_e^{ave} ($cm^2V^{-1}s^{-1}$)	V_{th}(V)	I_{on}/I_{off}	*SS* (V/decade)
PNDI2T-DTD[b]	1.52 (1.34 [d])	1.34 (1.18 [d])	30±4	10^4-10^5	8-10
PNDI2T-DT[b]	0.32 (0.22 [d])	0.23 (0.16 [d])	28±3	10^3	14-17
PNDI2T-DT (ref.)[c]	0.39	0.32	34.8	1.8×10^4	---

[a]Data from this work were obtained based on more than 30 devices. [b]Data from this work. [c]Data from previous report for bottom gate top-contact FETs on OTS-modified SiO_2/Si rigid substrate.[31] [d]The effective mobilities were calculated with the reliability factors (r_{sat}), which were calculated to be 0.88 and 0.68 for **PNDI2T-DTD** and **PNDI2T-D**T, respectively, on the basis of their respective device transfer curves.[45]

GIWAXS and AFM characterizations

The thermally annealed thin film of **PNDI2T-DTD** was characterized by grazing-incidence wide angle X-ray scattering (GIWAXS) and atomic force microscopy (AFM). **Figure 4** shows the two-dimensional GIWAXS pattern and the pole figures of **PNDI2T-DTD**, compiled by the integral intensities from (100) peaks in *out-of-plane* direction. The corresponding linecut profiles are provided in **Figure S5**. For comparison, the thin film of **PNDI2T-DT** was also investigated. In *out-of-plane* direction (**Figures 4a**, **4b**, and **S5**), (x00) scattering signals up to 5th order due to lamellar packing of side chains were observed for thin film of **PNDI2T-DTD**, and the corresponding *d*-spacing was calculated to be 23.2 Å. In comparison, only (100) and (200) scattering signals as well as a very dispersive (300) one with a *d*-spacing of 23.9 Å were observed for thin film of **PNDI2T-DT**. It is obvious that replacing branching chains with linear

ones as in **PNDI2T-DTD** can improve the lamellar packing order of side alkyl chains and shorten the lamellar packing *d*-spacing.

In *in-plane* direction (**Figures 4a**, **4b**, and **S5**), a broad and weak (010) signal at q_y = 1.65 Å^{-1} was observed for thin film of **PNDI2T-DTD** due to the interchain π–π packing of 3.8 Å. For thin film of **PNDI2T-DT**, a weak (010) scattering signal (q_z = 1.61 Å^{-1}), corresponding to a π–π stacking distance of 3.9 Å, was detected in *out-of-plane* direction. We also observed (100) and (200) scattering signals for both the polymers in the *in-plane* direction, indicating that both *edge-on* and *face-on* packing modes co-exist in the two polymer thin films. Pole figures based on (100) scattering signals (**Figure 4c-d**) were further constructed to calculate the ratios of the *edge-on* and *face-on* populations, and found as 12/1 and 4/1 for the thin films of **PNDI2T-DTD** and **PNDI2T-DT**, respectively. These results demonstrate that the polymer chains of **PNDI2T-DTD** adopt mainly *edge-on* packing mode on the substrate, whereas those of **PNDI2T-DT** adopt both *edge-on* (80%) and *face-on* (20%) orientations. It is noted that *edge-on* packing mode is known to be favorable for charge transporting in FET devices.[46] This may contribute to the fact that electron mobility of thin film of **PNDI2T-DTD** is higher than that of **PNDI2T-DT**. These results manifest that this side chain strategy can alter the interchain packing mode. The *edge-on* packing preference observed for **PNDI2T-DTD** is relevant to the pre-aggregation of the polymer chains in solution. The single polymer chain of **PNDI2T-DT** in well dissolved state is expected to lie flat (*face-on*) or stand up (*edge-on*) on the substrate randomly. However, in the case of **PNDI2T-DTD**, the pre-aggregates are more inclined to stand up on the substrate as reported previously.[47]

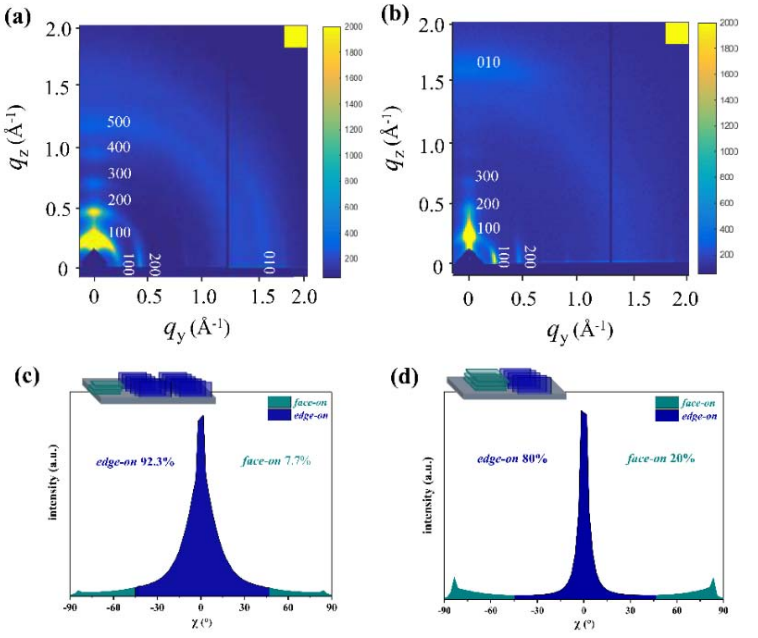

Figure 4. GIWAXS patterns of **PNDI2T-DTD** (a), **PNDI2T-DT** (b) and their *out-of-plane* and pole figures, compiled by the integral intensities from (100) peaks, of thin films of **PNDI2T-DTD** (c) and **PNDI2T-DT** (d) after thermal annealing at 160 ^{o}C; χ is defined as the angle between the crystallite orientation and the surface normal.

The thin films of **PNDI2T-DTD** and **PNDI2T-DT** were also characterized by AFM. As depicted in **Figure 5a**, **5c**, fibrous morphology is present in thin film of **PNDI2T-DT** with R_{RMS} (root-mean-square roughness) of 0.41 nm. However, after introducing linear chains, thin film of **PNDI2T-DTD** (**Figure 5b**, **5d)** displays grain-like morphology with R_{RMS} of 0.88 nm. Such morphology difference can be understood as follows. **PNDI2T-DT** exhibits good solubility because of the presence of two branching alkyl chains in each NDI unit. As a result, pre-aggregation of **PNDI2T-DT** cannot occur and the polymer chains tend to assemble into fibrous structures after evaporation of solvents with the spin-coating method, according to previous studies.[48] In comparison, **PNDI2T-DTD** shows poor solubility after replacing one branching

alkyl chain with the linear one. Thus, pre-aggregation of the polymer chains can occur, which agrees well with the absorption spectral studies as discussed above. Moreover, the linear alkyl chains in **PNDI2T-DTD** are favorable for the dense packing of polymer chains. The assembly of these pre-aggregates in solution of **PNDI2T-DTD** is anticipated to form grains within the spin-coated thin film.

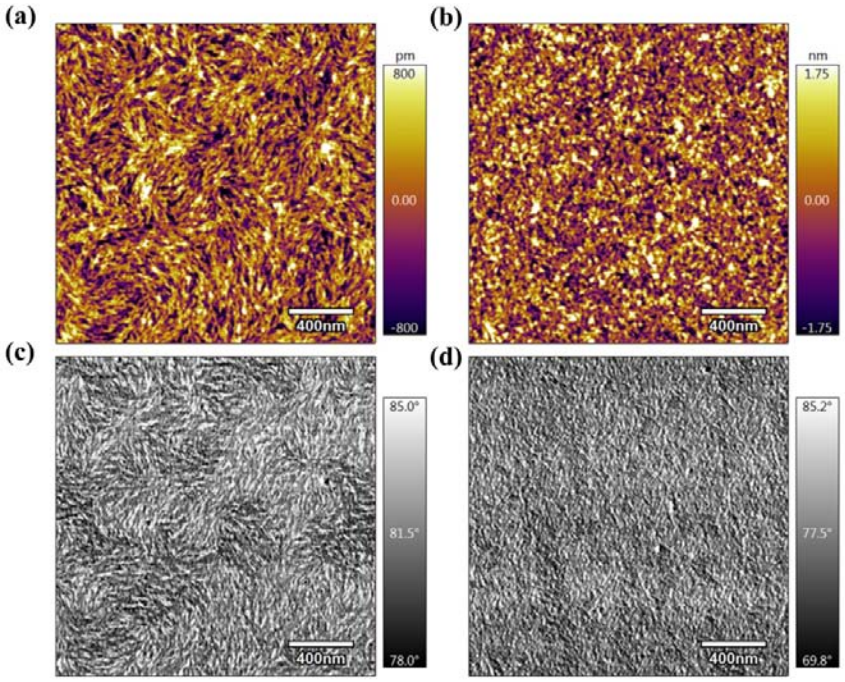

Figure 5. AFM height images and phase images (2 μm×2 μm) of the thin-films of **PNDI2T-DT** (a, c) and **PNDI2T-DTD** (b, d) after annealing at 160 °C.

Conclusion

In summary, we report a simple and efficient side-chain engineering strategy by partially replacing branching alkyl chains with linear ones in typical *n*-type NDI-bithiophene copolymer **PNDI2T-DTD**. By comparing with **PNDI2T-DT** in which the branching alkyl chains are connected to all NDI units, the thin film of **PNDI2T-DTD** shows improved lamellar packing of alkyl chains and the interchain π-π stacking distance is shortened, as revealed by the GIWAXS

data. Moreover, the absorption spectra at different temperatures reveal that the pre-aggregation of polymer chains of **PNDI2T-DTD** occurs in solution. As a result, the FET devices with thin films of **PNDI2T-DTD** on flexible PET substrates exhibit high electron mobility up to 1.52 $cm^2V^{-1}s^{-1}$. Furthermore, the devices show good air stability, and maximum electron mobility can remain to be 1.50 $cm^2V^{-1}s^{-1}$ after being left in air for 100 days. This study demonstrates the effectiveness of this side chain modification strategy, in which half of the branching alkyl chains are replaced by the linear ones, for improving thin film crystallinity, enhancing charge mobility and fabricating flexible FETs.

ASSOCIATED CONTENT

Supporting Information

Materials and Characterization techniques, Synthesis and characterization, TGA, DSC curves, Cyclic voltammograms, Solubility experiment, Linecut profiles, Device Fabrication and Measurements, Mechanical bending of flexible FETs, Performance data of flexible FETs with polymeric semiconductors, NMR data and Reference. This material is available free of charge via the Internet at http://pubs.acs.org.

AUTHOR INFORMATION

Corresponding Author

E-mail: dqzhang@iccas.ac.cn (D.Z.), drzitong@gmails.com (Z.L.)

Present Addresses

Beijing National Laboratory for Molecular Sciences, CAS Key Laboratory of Organic Solids, CAS Center of Excellence in Molecular Sciences, Institute of Chemistry, Chinese Academy of Sciences, Beijing, 100190, P. R. China

University of Chinese Academy of Sciences, Beijing 100049, P. R. China.

Author Contributions

[§]J.M and Z.Z contributed equally to this work.

Funding Sources

The Youth Innovation Promotion Association CAS (No. 2015024);

National Natural Science Foundation of China (21790360, 21661132006);

The Strategic Priority Research Program of the CAS (XDB12010300);

National Key R&D Program of China (2017YFA0204701).

Notes

The authors declare no competing financial interest.

ACKNOWLEDGMENT

We thank the financial support of the Youth Innovation Promotion Association CAS (No. 2015024), NSFC (21790360, 21661132006), the Strategic Priority Research Program of the CAS (XDB12010300), the National Key R&D Program of China (2017YFA0204701), The National Postdoctoral Program for Innovative Talents (BX201700254). We also thank Dr. Joseph Strzalka and Dr. Zhang Jiang for the assistance with GIWAXS measurements. Use of the Advanced Photon Source (APS) at Argonne National Laboratory was supported by the U.S. Department of Energy, Office of Science, Office of Basic Energy Sciences, under contract no. DE-AC02-06CH11357.

REFERENCES

(1) Someya, T.; Bao, Z.; Malliaras, G. G. The Rise of Plastic Bioelectronics. *Nature* **2016**, *540*, 379-385.

(2) Wang, B.; Huang, W.; Chi, L.; Al-Hashimi, M.; Marks, T. J.; Facchetti, A. High-*k* Gate Dielectrics for Emerging Flexible and Stretchable Electronics. *Chem. Rev.* **2018**, *118*, 5690-5754.

(3) Yan, H.; Chen, Z.; Zheng, Y.; Newman, C.; Quinn, J. R.; Dötz, F.; Kastler, M.; Facchetti, A. A High-Mobility Electron-Transporting Polymer for Printed Transistors. *Nature* **2009**, *457*, 679-686.

(4) Ha, Y-g; Jeong, S.; Wu, J.; Kim, M-G.; Dravid, V. P.; Facchetti, A.; Marks, T. J. Flexible Low-Voltage Organic Thin-Film Transistors Enabled by Low-Temperature, Ambient Solution-Processable Inorganic/Organic Hybrid Gate Dielectrics. *J. Am. Chem. Soc.* **2010**, *132*, 17426-17434.

(5) Sirringhaus, H. 25th anniversary article: Organic Field-Effect Transistors: The Path Beyond Amorphous Silicon. *Adv. Mater.* **2014**, *26*, 1319-1935.

(6) Sekitani, T.; Yokota, T.; Zschieschang, U.; Klauk, H.; Bauer, S.; Takeuchi, K. Takamiya, M.; Sakurai, T.; Someya, T. Organic Nonvolatile Memory Transistors for Flexible Sensor Arrays. *Science* **2009**, *326*, 1516-1519.

(7) Yamamoto, Y.; Harada, S.; Yamamoto, D.; Honda, W.; Arie, T.; Akita, S.; Takei, K. Printed Multifunctional Flexible Device with an Integrated Motion Sensor for Health Care Monitoring. *Sci. Adv.* **2016**, e1601473.

(8) Schwartz, G.; Tee, B. C.-K.; Mei, J.; Appleton, A. L.; Kim, D. H.; Wang, H.; Bao, Z. Flexible Polymer Transistors with High Pressure Sensitivity for Application in Electronic Skin and Health Monitoring. *Nat. Commun.* **2013**, *4*, 1859.

(9) Deng, W.; Zhang, X. J.; Zhang, X. H.; Guo, J. H.; Jie, J. S. Ordered and Patterned Assembly of Organic Micro/Nanocrystals for Flexible Electronic and Optoelectronic Devices. *Adv. Mater. Technol.* **2017**, *2*, 1600280.

(10) Li, M.; An, C.; Pisula, W.; Müllen, K. Cyclopentadithiophene-Benzothiadiazole Donor-Acceptor Polymers as Prototypical Semiconductors for High-Performance Field-Effect Transistors. *Acc. Chem. Res.* **2018**, *51*, 1196-1205.

(11) Wang, Y.; Guo, H.; Harbuzaru, A.; Uddin, M. A.; Arrechea-Marcos, I.; Ling, S.; Yu, J.; Tang, Y.; Sun, H.; López Navarrete, J. T.; Ortiz, R. P.; Woo, H. Y.; Guo, X. (Semi)ladder-Type Bithiophene Imide-Based All-Acceptor Semiconductors: Synthesis, Structure-Property Correlations, and Unipolar n-Type Transistor Performance. *J. Am. Chem. Soc.* **2018**, *140*, 6095-6108.

(12) Xin, H.; Ge, C.; Jiao, X.; Yang, X.; Rundel, K.; McNeill, C. R.; Gao, X. Incorporation of 2,6-Connected Azulene Units into the Backbone of Conjugated Polymers: Towards High-Performance Organic Optoelectronic Materials. *Angew. Chem. Int. Ed.* **2018**, *57*, 1322-1326.

(13) Xue, G.; Zhao, X.; Qu, G.; Xu, T.; Gumyusenge, A.; Zhang, Z.; Zhao, Y.; Diao, Y.; Li, H.; Mei, J. Symmetry Breaking in Side Chains Leading to Mixed Orientations and Improved Charge Transport in Isoindigo-alt-Bithiophene Based Polymer Thin Films. *ACS Appl. Mater. Interfaces* **2017**, 9, 25426-25433.

(14) Shi, K.; Zhang, W.; Gao, D.; Zhang, S.; Lin, Z.; Zou, Y.; Wang, L.; Yu, G. Well-Balanced Ambipolar Conjugated Polymers Featuring Mild Glass Transition Temperatures Toward High-Performance Flexible Field-Effect Transistors. *Adv. Mater.* **2018**, *30*, 1705286.

(15) Ni, Z.; Dong, H.; Wang, H.; Ding, S.; Zou, Y.; Zhao, Q.; Zhen, Y.; Liu, F.; Jiang, L.; Hu, W. Quinoline-Flanked Diketopyrrolopyrrole Copolymers Breaking through Electron Mobility over 6 cm^2V^{-1} s^{-1} in Flexible Thin Film Devices. *Adv. Mater.* **2018**, *30*, 1704843.

(16) Shi, Y.; Guo, H.; Qin, M.; Zhao, J.; Wang, Y.; Wang, H.; Wang, Y.; Facchetti, A.; Lu, X.; Guo, X. Thiazole Imide-Based All-Acceptor Homopolymer: Achieving High-Performance Unipolar Electron Transport in Organic Thin-Film Transistors. *Adv. Mater.* **2018**, *30*, 1705745.

(17) Li, H.; Kim, F. S.; Ren, G.; Jenekhe, S. A. High-Mobility n-Type Conjugated Polymers Based on Electron-Deficient Tetraazabenzodifluoranthene Diimide for Organic Electronics. *J. Am. Chem. Soc.* **2013**, *135*, 14920-14923.

(18) Liu, X.; He, B.; Garzón-Ruiz, A.; Navarro, A.; Chen, T. L.; Kolaczkowski, M. A.; Feng, S.; Zhang, L.; Anderson, C. A.; Chen, J.; Liu, Y. Unraveling the Main Chain and Side Chain Effects on Thin Film Morphology and Charge Transport in Quinoidal Conjugated Polymers. *Adv. Funct. Mater.* **2018**, *28*, 1801874.

(19) Zhao, Y.; Gumyusenge, A.; He, J.; Qu, G.; McNutt, W. W.; Long, Y.; Zhang, H.; Huang, L.; Diao, Y.; Mei, J. Continuous Melt-Drawing of Highly Aligned Flexible and Stretchable Semiconducting Microfibers for Organic Electronics. *Adv. Funct. Mater.* **2018**, *28*, 1705584.

(20) Chen, M. S.; Lee, O. P.; Niskala, J. R.; Yiu, A. T.; Tassone, C. J.; Schmidt, K.; Beaujuge, P. M.; Onishi, S. S.; Toney, M. F.; Zettl, A.; Fréchet, J. M. Enhanced Solid-State Order and Field-Effect Hole Mobility through Control of Nanoscale Polymer Aggregation. *J. Am. Chem. Soc.* **2013**, *135*, 19229-19236.

(21) Virkar, A. A.; Mannsfeld, S.; Bao, Z.; Stingelin, N. Organic Semiconductor Growth and Morphology Considerations for Organic Thin-Film Transistors. *Adv. Mater.* **2010**, *22*, 3857-3875.

(22) Fei, Z.; Han, Y.; Martin, J.; Scholes, F. H.; Al-Hashimi, M.; AlQaradawi, S. Y.; Stingelin, N.; Anthopoulos, T. D.; Heeney, M. Conjugated Copolymers of Vinylene Flanked Naphthalene Diimide. *Macromolecules* **2016**, *49*, 6384-6393.

(23) Sun, B.; Hong, W.; Yan, Z.; Aziz, H.; Li, Y. Record High Electron Mobility of 6.3 $cm^2 V^{-1} s^{-1}$ Achieved for Polymer Semiconductors Using a New Building Block. *Adv. Mater.* **2014**, *26*, 2636-2642.

(24) Erdmann, T.; Fabiano, S.; Milian-Medina, B.; Hanifi, D.; Chen, Z.; Berggren, M.; Gierschner, J.; Salleo, A.; Kiriy, A.; Voit, B.; Facchetti, A. Naphthalenediimide Polymers with Finely Tuned In-Chain π-Conjugation: Electronic Structure, Film Microstructure, and Charge Transport Properties. *Adv. Mater.* **2016**, *28*, 9169-9174.

(25) Zhang, D.; Zhao, L.; Zhu, Y.; Li, A.; He, C.; Yu, H.; He, Y.; Yan, C.; Goto, O.; Meng, H. Effects of p-(Trifluoromethoxy)benzyl and p-(Trifluoromethoxy)phenyl Molecular Architecture on the Performance of Naphthalene Tetracarboxylic Diimide-Based Air-Stable n-Type Semiconductors. *ACS Appl. Mater. Interfaces* **2016**, *8*, 18277-18283.

(26) Szumilo, M. M.; Gann, E. H.; McNeill, C. R.; Lemaur, V.; Oliver, Y.; Thomsen, L.; Vaynzof, Y.; Sommer, M.; Sirringhaus, H. Structure Influence on Charge Transport in Naphthalenediimide–Thiophene Copolymers. *Chem. Mater.* **2014**, *26*, 6796-6804.

(27) Nakano, M.; Osaka, I.; Takimiya, K. Naphthodithiophene Diimide (NDTI)-Based Semiconducting Copolymers: From Ambipolar to Unipolar n-Type Polymers. *Macromolecules* **2015**, *48*, 576-584.

(28) He, T.; Stolte, M.; Würthner, F. Air-Stable n-Channel Organic Single Crystal Field-Effect Transistors Based on Microribbons of Core-Chlorinated Naphthalene Diimide. *Adv. Mater.* **2013**, *25*, 6951-6955.

(29) Hillebrandt, S.; Adermann, T.; Alt, M.; Schinke, J.; Glaser, T.; Mankel, E.; Hernandez-Sosa, G.; Jaegermann, W.; Lemmer, U.; Pucci, A.; Kowalsky, W.; Müllen, K.; Lovrincic, R.; Hamburger, M. Naphthalene Tetracarboxydiimide-Based n-Type Polymers with Removable Solubility via Thermally Cleavable Side Chains. *ACS Appl. Mater. Interfaces* **2016**, *8*, 4940-4945.

(30) Kim, Y.; Long, D. X.; Lee, J.; Kim, G.; Shin, T. J.; Nam, K.-W.; Noh, Y.-Y.; Yang, C. A Balanced Face-On to Edge-On Texture Ratio in Naphthalene Diimide-Based Polymers with Hybrid Siloxane Chains Directs Highly Efficient Electron Transport. *Macromolecules* **2015**, *48*, 5179-5187.

(31) Lee, W.; Lee, C.; Yu, H.; Kim, D.-J.; Wang, C.; Woo, H. Y.; Oh, J. H.; Kim, B. J. Side Chain Optimization of Naphthalenediimide-Bithiophene-Based Polymers to Enhance the Electron Mobility and the Performance in All-Polymer Solar Cells. *Adv. Funct. Mater.* **2016**, *26*, 1543-1553.

(32) Yang, J.; Xiao, B.; Heo, S. W.; Tajima, K.; Chen, F.; Zhou, E. Effects of Inserting Thiophene as a pi-Bridge on the Properties of Naphthalene Diimide-alt-Fused Thiophene Copolymers. *ACS Appl. Mater. Interfaces* **2017**, *9*, 44070-44078.

(33) Wang, Y.; Hasegawa, T.; Matsumoto, H.; Mori, T.; Michinobu, T. D-A_1-D-A_2 Backbone Strategy for Benzobisthiadiazole Based n-Channel Organic Transistors: Clarifying the Selenium-Substitution Effect on the Molecular Packing and Charge Transport Properties in Electron-Deficient Polymers. *Adv. Funct. Mater.* **2017**, *27*, 1701486.

(34) Zhao, Z.; Yin, Z.; Chen, H.; Zheng, L.; Zhu, C.; Zhang, L.; Tan, S.; Wang, H.; Guo, Y.; Tang, Q.; Liu, Y. High-Performance, Air-Stable Field-Effect Transistors Based on Heteroatom-

Substituted Naphthalenediimide-Benzothiadiazole Copolymers Exhibiting Ultrahigh Electron Mobility up to 8.5 $cm^2 V^{-1} s^{-1}$. *Adv. Mater.* **2017**, *29*, 1602410.

(35) Wang, Y.; Hasegawa, T.; Matsumoto, H.; Mori, T.; Michinobu, T. High-Performance n-Channel Organic Transistors Using High-Molecular-Weight Electron-Deficient Copolymers and Amine-Tailed Self-Assembled Monolayers. *Adv. Mater.* **2018**, *30*, 1707164.

(36) Steyrleuthner, R.; Di Pietro, R.; Collins, B. A.; Polzer, F.; Himmelberger, S.; Schubert, M.; Chen, Z.; Zhang, S.; Salleo, A.; Ade, H.; Facchetti, A.; Neher, D. The Role of Regioregularity, Crystallinity, and Chain Orientation on Electron Transport in a High-Mobility n-Type Copolymer. *J. Am. Chem. Soc.* **2014**, *136*, 4245-4256.

(37) Kang, B.; Kim, R.; Lee, S. B.; Kwon, S. K.; Kim, Y. H.; Cho, K. Side-Chain-Induced Rigid Backbone Organization of Polymer Semiconductors through Semifluoroalkyl Side Chains. *J. Am. Chem. Soc.* **2016**, *138*, 3679-3686.

(38) Kim, R.; Amegadze, P. S. K.; Kang, I.; Yun, H.-J.; Noh, Y.-Y.; Kwon, S.-K.; Kim, Y.-H. High-Mobility Air-Stable Naphthalene Diimide-Based Copolymer Containing Extended π-Conjugation for n-Channel Organic Field Effect Transistors. *Adv. Funct. Mater.* **2013**, *23*, 5719-5727.

(39) Sung, M. J.; Luzio, A.; Park, W.-T.; Kim, R.; Gann, E.; Maddalena, F.; Pace, G.; Xu, Y.; Natali, D.; de Falco, C.; Dang, L.; McNeill, C. R.; Caironi, M.; Noh, Y.-Y.; Kim, Y.-H. High-Mobility Naphthalene Diimide and Selenophene-Vinylene-Selenophene-Based Conjugated Polymer: n-Channel Organic Field-Effect Transistors and Structure-Property Relationship. *Adv. Funct. Mater.* **2016**, *26*, 4984-4997.

(40) Li, M.; An, C.; Marszalek, T.; Baumgarten, M.; Yan, H.; Müllen, K.; Pisula, W. Controlling the Surface Organization of Conjugated Donor-Acceptor Polymers by their Aggregation in Solution. *Adv. Mater.* **2016**, *28*, 9430-9438.

(41) Kim, N.-K.; Jang, S.-Y.; Pace, G.; Caironi, M.; Park, W.-T.; Khim, D.; Kim, J.; Kim, D.-Y.; Noh, Y.-Y. High-Performance Organic Field-Effect Transistors with Directionally Aligned Conjugated Polymer Film Deposited from Pre-Aggregated Solution. *Chem. Mater.* **2015**, *27*, 8345-8353.

(42) Nahid, M. M.; Welford, A.; Gann, E.; Thomsen, L.; Sharma, K. P.; McNeill, C. R. Nature and Extent of Solution Aggregation Determines the Performance of P(NDI2OD-T2) Thin-Film Transistors. *Adv. Electron. Mater*. **2018**, *4*, 1700559.

(43) Cheng, C.; Geng, H.; Yi, Y.; Shuai, Z. Super-Exchange-Induced High Performance Charge Transport in Donor–Acceptor Copolymers. *J. Mater. Chem. C* **2017**, *5*, 3247-3253.

(44) Ashraf, R. S.; Chen, Z.; Leem, D. S.; Bronstein, H.; Zhang, W.; Schroeder, B.; Geerts, Y.; Smith, J.; Watkins, S.; Anthopoulos, T. D.; Sirringhaus, H.; de Mello, J. C.; Heeney, M.; McCulloch, I. Silaindacenodithiophene Semiconducting Polymers for Efficient Solar Cells and High-Mobility Ambipolar Transistors. *Chem. Mater.* **2011**, *23*, 768-770.

(45) Choi, H. H.; Cho, K.; Frisbie, C. D.; Sirringhaus, H.; Podzorov, V. Critical Assessment of Charge Mobility Extraction in FETs. *Nature. Mater.* **2017**, *17*, 2-7.

(46) Chen, H. -Y.; Hou, J.; Hayden, A. E.; Yang, H.; Houk, K. N.; Yang, Y. Silicon Atom Substitution Enhances Interchain Packing in a Thiophene-Based Polymer System. *Adv. Mater.* **2010**, *22*, 371-375.

(47) Wang, Z.; Liu, Z.; Ning, L.; Xiao, M.; Yi, Y.; Cai, Z.; Sadhanala, A.; Zhang, G.; Chen, W.; Sirringhaus, H.; Zhang, D. Charge Mobility Enhancement for Conjugated DPP-Selenophene

Polymer by Simply Replacing One Bulky Branching Alkyl Chain with Linear One at Each DPP Unit. *Chem. Mater.* **2018**, *30*, 3090-3100.

(48) Li, W.; Hendriks, K. H.; Furlan, A.; Roelofs, W. S.; Meskers, S. C.; Wienk, M. M.; Janssen, R. A. Effect of the Fibrillar Microstructure on the Efficiency of High Molecular Weight Diketopyrrolopyrrole-Based Polymer Solar Cells. *Adv. Mater.* **2014**, *26*, 1565-1570.

Table of Contents